Journal of Applied Fluid Mechanics, Vol. 18, No. 11, pp. 2742-2756, 2025.
Available online at www.jafmonline.net, ISSN 1735-3572, EISSN 1735-3645.
https://doi.org/10.47176/jafm.18.11.3553

Prediction of Energy Dissipation and Length of Jump over Modified Stepped Spillway using Empirical and Adaptive Neuro-fuzzy Inference System Technique

P. Dharmadhikari †and S. Gandhi

Department of Civil Engineering, Jaypee University of Engineering and Technology Guna, Guna, India

†*Corresponding Author Email: 213d001@juetguna.in*

ABSTRACT

This study aims to enhance energy dissipation efficiency by introducing an alternative design to conventional stepped spillways. To achieve this, modified stepped spillway (MSS) with reflector were used and analyzed experimentally for energy dissipation and length of jump. Empirical models were developed to characterize the hydraulic jump with good R^2 values of 0.86, 0.96 and 0.86 for sequent depth ratio, relative energy loss and relative length of jump respectively. Results indicate jump characteristics are greatly influenced by curved steps, flow regime and turbulence. Higher Froude number increases roller length, jump length and energy loss. Adaptive Neuro-Fuzzy Inference System (ANFIS) model is also utilized for modified stepped spillway to predict flow characteristics for training and validation of experimental results. It is found that ANFIS predicts the non-linear transition effectively by achieving RMSE, R^2 and MSE training values as 0.06, 0.98 and 0.43 respectively, which are a favorable performance metrics. 3D surface plot provides thorough understanding of parametric dependencies facilitating the identification of key input factors that influence hydraulic modeling. All three models are found to be capable of optimizing the flow and efficient in controlling the length of roller and length of jump. It is concluded that stepped spillways with reflectors and higher number of steps have more energy dissipation rates at various discharge. Also, ANFIS can be trained with experimental or field data, allowing it to adapt to specific site conditions for design configurations.

Article History

Received April 1, 2025
Revised June 16, 2025
Accepted June 17, 2025
Available online September 3, 2025

Keywords:

Stepped spillway
Reflectors
Energy loss
Length of jump
Empirical modeling
Adaptive Neuro-Fuzzy Inference System Technique (ANFIS)

1. INTRODUCTION

Modified stepped spillways (MSS) with reflector are an innovative adaptation of traditional stepped spillways, designed to enhance the energy dissipation capabilities of hydraulic structures. However, the standard stepped spillway design has limitations in achieving optimal energy dissipation, particularly under varying hydraulic conditions. MSS introduces a circular geometry to the steps, creating a distinctive flow pattern that improves turbulence and energy dissipation. This design modification seeks to address the challenges of conventional flat steps by optimizing the interaction between flowing water and the spillway surface. By altering the step shape, the MSS enhances flow resistance and turbulence generation, thereby improving the overall hydraulic performance. While many researchers consider the effects of aerated flows, the main goal of using MSS is to create disturbances within the steps, leading to backwater effects and turbulence that enhance aeration. Since such type of flow is resulting in higher critical depth to step height ratio than simple stepped spillway, it becomes more effective in energy dissipation.

The energy dissipation over stepped spillways with step numbers and dimension was studied by authors like Roushangar et al. (2014) and Ghaderi et al. (2020); the findings indicate that more is the steps, the greater is energy dissipation. Daneshfaraz et al. (2024) emphasized flow simulation accuracy and processing efficiency in his study while using finite element volume technique. In order to anticipate the relative energy in terms of non-dimensional characteristics such as baffle dimension and spillway relative height, Nasralla (2021) suggested an empirical equation utilizing multivariate regression analysis. According to Salmasi and Abraham (2022) experimental investigation with differing slopes and steps, the impact of spillway slope and step count on the rate of energy dissipation is minimal. However, data driven approach have been

NOMENCLATURE

E_1	energy per unit weight at section 1 (before the jump)	Y_1	prejump depth
E_2	energy per unit weight at section 2 (after the jump)	Y_2	postjump depth
E_L	energy loss per unit weight ($E_1 - E_2$)	y_c	critical depth of flow
F_{r1}	approach Froude number	Y_2/Y_1	sequent depth ratio
L_r	length of roller	E_L/E_1	relative energy loss
L_j	length of roller	L_j/Y_1	relative length of jump
n	number of steps	L_r/Y_2	relative length of roller
Q	discharge	ρ	density of water
R_{e1}	Reynold's number	υ	kinematic viscosity
r	radius of curve spillway	ε	surface roughness
V_1	velocity at section 1	μ	dynamic viscosity of water
V_2	velocity at section 2		

followed by Nouri et al. (2020) , Kordnaeij et al. (2023) and Alashan et al. (2023) for energy dissipation in stepped spillways but there is scarcity of literature for MSS.

In contrast to widely used parametric statistical methods, ANFIS enable the creation of models without requiring a significant understanding of the distribution of the data population or the possible interaction effects between variables. Given the aforementioned significance of MSS, the primary focus of the current study is to analyze energy dissipation and reduction in the length of jump. Nishank and Ellora (2025) selected the best model for jump length calculation using two different approaches, namely Levenberg-Marquardt method and gradient descent with momentum and adaptive learning rule back propagation method.

As highlighted, numerous researchers have focused on optimizing step geometry to enhance energy dissipation on spillways. In this study, circular step geometry (MSS) is considered, offering the potential for greater energy dissipation through lower back water generation. Application of ANFIS provides the additional benefit of interpretability and robustness due to its fuzzy logic foundation outperforming the existing empirical equations.

2. RESEARCH THEORY

Extensive research on energy dissipation mechanisms with notable contributions from scholars like Rajaratnam (1990), Chanson (1994) and Pegram et al. (1999) were well reported for stepped spillways. Authors have primarily been studied to establish design criteria and develop fundamental equations (Boes & Hager 2003). For instance, few researchers have investigated the flow characteristics of stepped spillways using box gabions (Zuhaira et al., 2020; Wuthrich & Chanson 2015). Additionally, other studies have focused on evaluating the extent of downstream scouring caused by stepped spillways (Aminpour & Farhoudi 2017; Eghlidi et al. 2020). Boes and Hager (2003) enlighten the benefits of stepped spillways with reduced cavitation risks and possibilities of smaller stilling basins. Investigations of energy dissipation over different forms of stepped spillways were conducted by Mero and Mitchell (2017). Their work supports the importance of tailoring stepped spillway designs to specific hydraulic conditions for enhanced efficiency and safety.

2.1 Research Gap and Novelty

This research effectively combines experimental analyses with ANFIS to estimate the hydraulic properties of MSS. The novelty of the research is as follows for less available literature in MSS with reflectors:

- First to understand the flow characteristics for Y_2/Y_1, E_L/E_1, L_j/Y_1 and L_r/Y_2, experiments were conducted with three different MSS models (Table 1). Then, empirical models were developed which is applicable for nappe flow (low velocity flow) as well as for skimming flow (high velocity flow).
- For deeper comprehension, integration of ANFIS and experimental methods for the investigation of energy loss (E_L/E_1) and length of jump (L_j/Y_1) were carried out with dataset that was acquired through experimentation.
- The study also highlights the potential of soft computing tools to optimize spillway design and performance monitoring, offering a robust framework for future research and practical applications.

2.2 Research Background of Energy Dissipation

Daneshfaraz et al. (2024) explored the influence of step configurations and step heights on energy dissipation capacity. Ikinciogullari (2021) employed software to quantitatively analyze the energy dissipation performance of trapezoidal stepped spillways, demonstrating an efficiency improvement of up to 30% compared to conventional designs. In 2023, Ikinciogullari introduced the MSS and performed numerical simulations to compare its energy dissipation rate against simple stepped spillways. The results revealed that smaller step radii enhance the MSS's performance. Similarly, Albank and Khassaf (2023) examined energy dissipation in stepped spillways with downstream angles of 25˚, 35˚ and 45˚, finding that pooling steps yielded 4.6% greater relative energy loss than flat steps. Al-Husseini et al. (2019) observed that reducing the number of steps and decreasing the downstream slope increased the energy dissipation

Table 1 Geometrical features of MSS models

Model	Step Geometry				
	Number of steps (n_s)	Step width (S_w cm)	Step length (S_L cm)	Step height (S_h cm)	Spillway radius (r cm)
Model-1	7	19.5	4	2.5	2.5
Model-2	4	19.5	4	3.1	2.5
Model-3	4	19.5	3.7	3.5	2.5

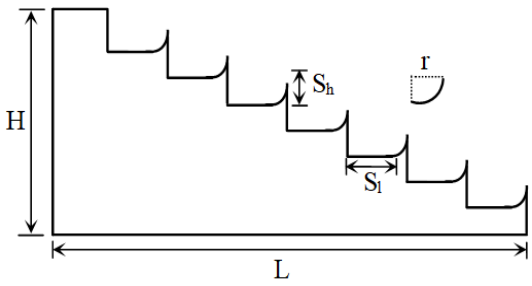

Fig. 1 Spillway model geometry and dimensions

efficiency of stepped spillways compared to flat-sloped ones. Asadi et al. (2015) experimentally demonstrated that the energy dissipation rate is influenced upto 4–11% by factors like discharge, sill height, and step length. Mero and Mitchell (2017) investigated the effect of modified step dimensions with reflectors on energy dissipation using different spillway configuration. The findings revealed that stepped spillways equipped with reflectors achieved significantly higher energy dissipation rates compared to conventional designs.

2.3 Research Background of ANFIS Technique

Conventional numerical methods used to analyze hydraulic jumps can be computationally demanding and often require extensive experimental data. The Adaptive Neuro-Fuzzy Inference System (ANFIS) has emerged as a valuable tool for modeling complex phenomena for flow over stepped spillways. ANFIS, by integrating fuzzy logic with neural networks, offers an efficient alternative for predicting flow characteristics with notable accuracy. Several studies have demonstrated the efficacy of ANFIS, for instance Mojtahedi et al. (2020) applied ANFIS to model energy dissipation over stepped spillways, achieving results that aligned closely with experimental data. Similarly, Roushangar et al. (2014) utilized ANFIS to predict flow behavior over stepped spillways, highlighting its superiority over traditional regression models in capturing nonlinear interactions. Furthermore, Zounemat-Kermani et al. (2013) employed ANFIS to estimate air demand in dam bottom outlets, underscoring its versatility in various hydraulic applications. These studies collectively underscore ANFIS's potential to enhance the design and optimization of stepped spillways, leading to more efficient hydraulic structures.

3. Fabrication Of Spillway Model

Ohtsu et al. (2004) describe two flow regimes namely nappe and skimming flow regimes under different flow condition with stepped spillway. In this transitional phase, the flow no longer exhibits the typical characteristics of nappe flow as well as adopts the traits of skimming flow. However, this phase is challenging for designers due to the heightened vibrations it generates, as noted by Chanson (1996). Chanson (2001) and Boes and Hager (2003) defined the upper and lower boundaries for flow by giving due weightage to step height, step length and critical flow depth. Authors conducted the studies for the discharge ranges between 0.0121 to 0.00684 m^3/s.

Three different wooden MSS models were fabricated and installed with the open channel flume one by one at the hydraulics laboratory (Table 1). Figure 1 shows spillway model geometry and dimensions of step. The number of steps is selected based on a combination of achieving the desired flow regime (nappe or skimming) with accommodating the spillway slope and step height. The step geometry depends upon S_h/S_l and y_c/S_h ratios (Chanson, 2001; Boes & Hager, 2003). The purpose of considering wooden material is to minimize the frictional effect even at low velocity of flow. Its edges are made curved with radius ‘r’ using aluminum sheet to behave as reflectors for the flow. These reflectors are responsible for generating back water flow regime at lower nappe of stream at each step. Symmetric flow formation and reduced erosion risks at all discharge value were the main objective while selecting the aluminum material.

4. Experimentation And Data Acquisition

The investigation of flow characteristics were carried out at the Hydraulics Laboratory of Jaypee University of Engineering and Technology Guna, MP, India. The experimental trials utilized a rectangular flume measuring 5 m in length, 0.20 m in width, and 0.25 m in height. This recirculating open channel flume supported flow velocities ranging from 0.8 m/s to 2 m/s and consisted of three main components as inlet section, outlet section and downstream collecting tank for discharge monitoring. Experiments were conducted for aforementioned characteristics (Y_2/Y_1, E_L/E_1, L_j/Y_1 and L_r/Y_2) for Froude number varying between 1 to 7 and Reynold’s number between 21.21 x 10^4 to 18.36 x 10^5. A pitot static tube, paired with a manometer, was used to determine mean velocities at the upstream and downstream sections. Pointer gauge were employed to measure depths at specified locations. In cases of fluctuating water surface profiles, depth measurements were averaged across multiple readings.

Flow into the channel was supplied via a pump equipped with a regulating valve, delivering water through an inlet tank designed to maintain a consistent flow. Discharge at the outlet was measured by volumetric

Table 2 Summary of measured and variable parameters

Model	Model-1	Model-2	Model-3	Mean	Median
Y_1 (m)	0.019-0.080	0.012-0.039	0.010-0.053	0.05	0.029
Y_2 (m)	0.077-0.11	0.050-0.120	0.048-0.180	0.084	0.09
Q (m^3/s)	0.005-0.033	0.005-0.011	0.003-0.021	0.018	0.009
F_{r1}	1-7	1-7	1-7	4	2.88
L_r (m)	0.159-0.588	0.171-0.580	0.210-0.600	0.379	0.36
L_j (m)	0.440-0.990	0.500-0.920	0.460-0.990	0.715	0.73
Y_2/Y_1	1.3-4.4	2.0-5.6	1.405-7.80	4.55	3.009
E_L/E_1	0.006-0.781	0.006-0.747	0.001-0.700	0.391	0.471
L_j/Y_1	8.5-31.5	12.8-54.9	16.05-83.64	46.07	25.145
L_r/Y_2	1.66-6.61	2.48-5.66	1.90-7.59	4.625	4.102

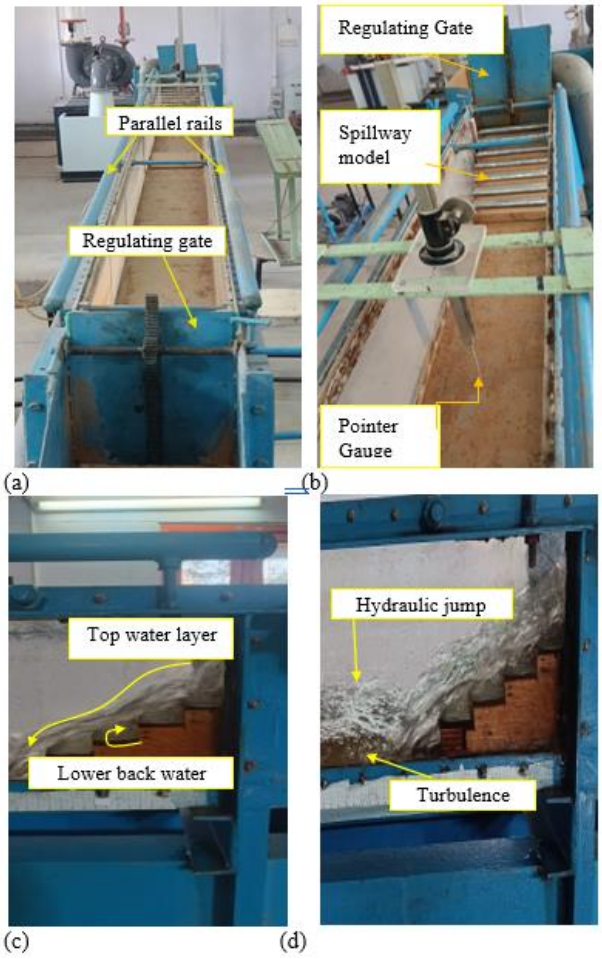

Fig. 2 (a) – (b) Instrumentation with spillway model, (c) - (d) Formation of jump and turbulence characteristics

method using the collection tank. Flume walls were made of perspex sheets, allowed for visualization of the flow profile on both sides. Efforts were taken to minimize side-wave reflection and surface undulations, ensuring stable flow conditions. Water entered the constant head input tank (dimensions: 35.5 × 49.0 × 44.0 cm³) through a 7.6 cm diameter pipe with a regulating valve to maintain uniform flow. Discharge was adjusted across a range to collect data for different approach Froude numbers. Sharp-edged control gates were placed upstream and downstream of the flume to locate the jump

Table 3 R^2 values of different flow characteristics

Model	Y_2/Y_1	E_L/E_1	L_j/Y_1	L_r/Y_2
Model-1	0.8906	0.9735	0.8498	0.635
Model-2	0.8955	0.9669	0.8602	0.571
Model-3	0.9036	0.943	0.8791	0.8127

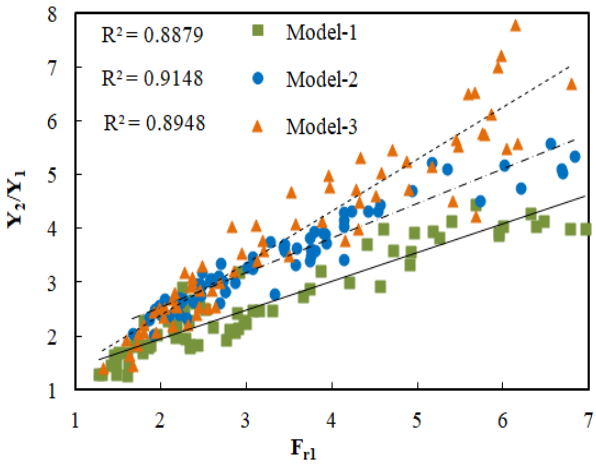

Fig. 3 Variation of Y_2/Y_1 against F_{r1}

formation during different trials. Eddy formation and surface rollers formation were optimized with smooth channel bed. Parallel rails were mounted to support pointer gauge for depth measurements at different points along the channel and across the channel width. During data collection, careful attention was paid to surface rollers and extreme turbulence. Efforts are made to ensure precise and reliable experimental results included minimizing water losses, maintaining symmetrical flow, and measuring depths at three specific locations along the channel. Figure 2(a)-(d) illustrate the experimental setup and sectional view of experimental setup. Detailed geometrical features of the spillway models, along with summaries of measured and variable parameters, are provided in Tables 1 and 2. Table 3 shows R^2 values for various jump characteristics.

Figure 3 illustrates that the sequent depth ratio (Y_2/Y_1) varies linearly with the approach Froude number (F_{r1}), ranging from 1 to 7 across all three models. This linear trend is supported by previous studies (Felder & Chanson, 2011; Eltoukhy, 2016; Simsek et al., 2023) and is consistent with the U.S. Bureau of reclamation

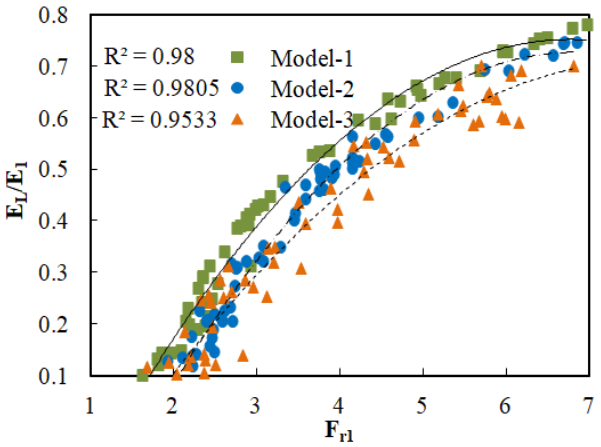

Fig. 4 Variation of E_L/E_1 against F_{r1}

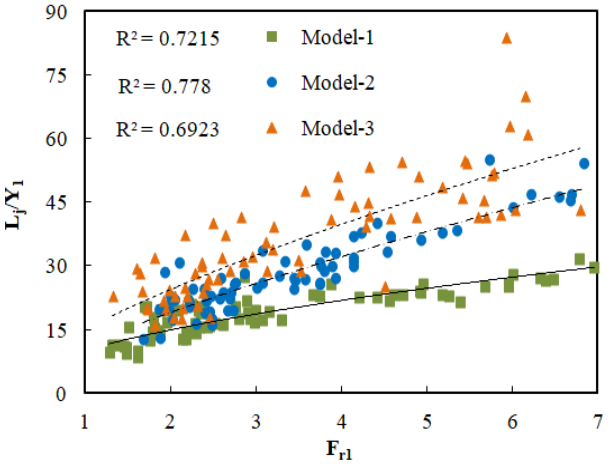

Fig. 5 Variation of L_j/Y_1 against F_{r1}

guidelines (1955, 1957) for Froude numbers between 4.5 and 9. Approximately 89% of the data points fall within ±10% of the best-fit line, with deviations likely due to potential inaccuracies in depth measurements.

Figure 4 illustrates an increasing trend in relative energy loss (E_L/E_1) with the Froude number (F_{r1}). The relationship between these variables is influenced by factors such as curvature, flow regime, and turbulence. Both experimental data and theoretical analysis highlight the effectiveness of circular stepped spillways in dissipating energy and enhancing structural stability. Studies by Parsamehr et al. (2023) and Parsaie et al. (2022), along with Chanson (2011), indicate that stepped spillways, including curved designs, effectively dissipate energy, exhibiting a transition from linear to nonlinear trends in energy loss (E_L/E_1) as F_{r1} increases. Similarly, Saghebian (2018) and Saurabh et al. (2023) observed that higher Froude numbers lead to more chaotic hydraulic jumps, resulting in increased energy dissipation. Their findings emphasize the significance of considering both channel slope and Froude number when predicting energy loss.

Figure 5 illustrates a nonlinear variation in the relative jump length (L_j/Y_1) against the approach Froude number (F_{r1}), ranging from 1 to 7 for all spillway arrangements. The logarithmic trend shows a low R^2

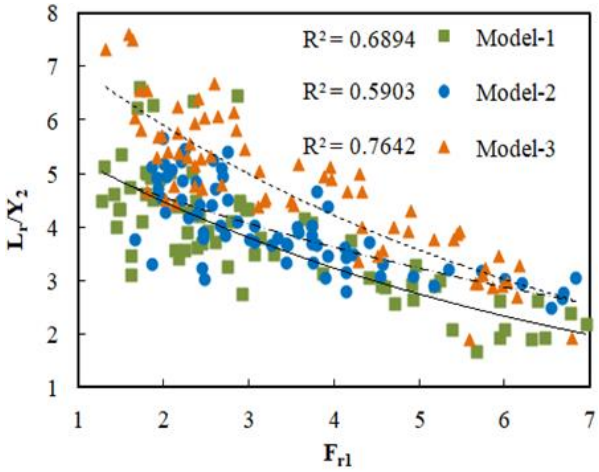

Fig. 6 Variation of L_r/Y_2 against F_{r1}

value, likely due to measurement challenges caused by turbulence, rollers, and eddies, making it difficult to pinpoint the exact start and end of the jump. The roller length, being shorter than the total jump length, is also hard to determine. Theoretically and experimentally, the jump length is typically 5 to 7 times the jump height in spillway designs. Similar conclusions were drawn by Yu et al. (2021) and Nikmehr and Aminpour (2020). Additionally, Elshaarawy and Hamed (2025) found that increased roughness reduces jump length, emphasizing the impact of bed roughness and upstream Froude number on hydraulic jump behavior.

Figure 6 shows the variation of relative length of roller (L_r/Y_2) with Froude number (F_{r1}) affects energy dissipation, flow stability, and hydraulic structure design. Higher F_{r1} generally increases roller length, enhancing energy loss and aeration, while rougher beds reduce it. Studies like Djamaa et al. (2020) and Elshaarawy and Hamed (2025) highlight its role in erosion control and stilling basin efficiency.

5. EMPIRICAL MODELING

Numerous empirical models for flow properties exist in the literature, such as those by Bushra and Afzal (2006) and Rajaratnam (1990), which emphasize Reynold's number as a critical factor influencing flow behavior. Pegram et al. (1999) further explored these models, illustrating their effectiveness in identifying the impact of drag on hydraulic jump phenomena. Key variables affecting flow characteristics in a circular channel includes Y_1, Y_2, V_1, V_2, E_1, E_2, L_r, L_j, μ, g, ρ, ε, S_l, S_h and n_s. Here 'Y_1' is prejump depth (m), 'Y_2' is post jump depth (m), 'V_1' is prejump velocity (m/s), 'V_2' is post jump velocity (m/s), 'L_r' is length of roller (m), 'L_j' is length of jump (m), 'μ' is dynamic viscosity of water (Ns/m^2), 'g' acceleration due to gravity (m/s^2), 'ρ' is density of water (Kg/m^3), 'ε' is surface roughness (m), 'S_l' is step length (m), 'S_h' is step height (m) and 'n_s' is number of steps. As shown in eqn. (1), these variables can be defined as functions involving both dependent and independent parameters.

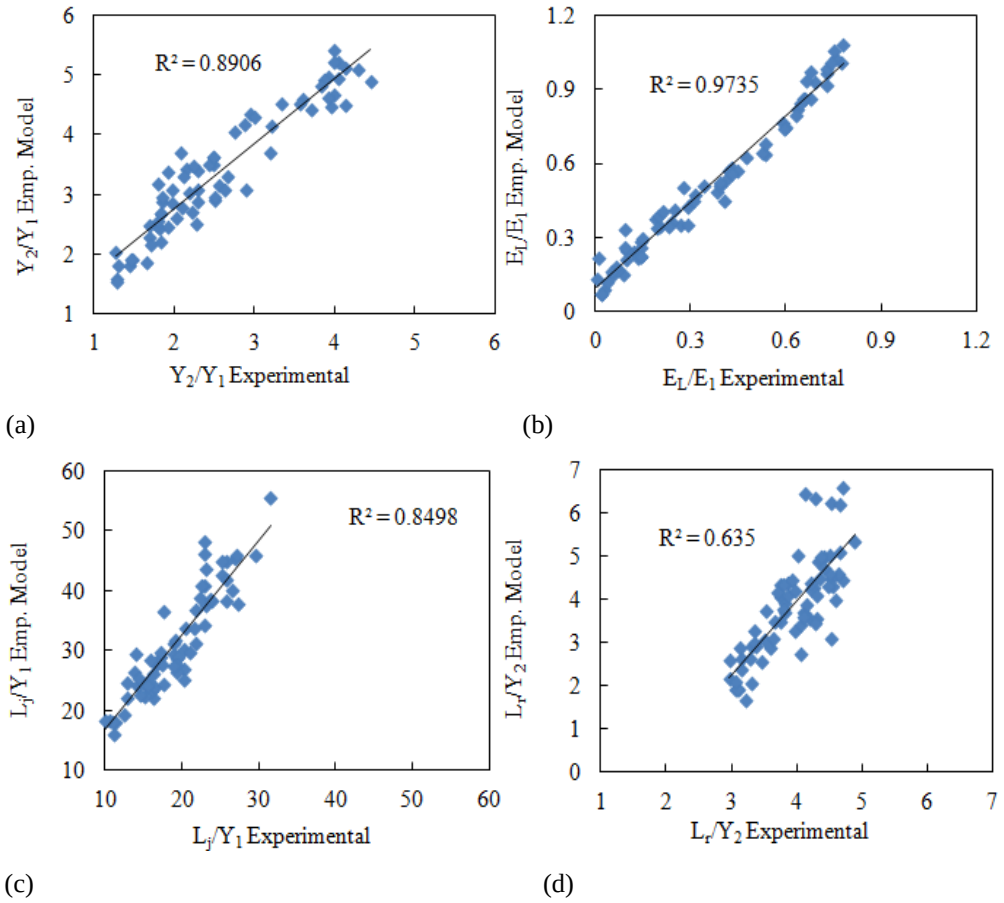

Fig. 7 (a) - (d) Empirical models and their linear fit for model-1

$$f\left(Y_1, Y_2, V_1, V_2, E_1, E_2, L_r, L_j, \mu, g, \rho, \varepsilon, S_l, S_h, H, r\right)=0 \quad (1)$$

The dimensionless groups can be represented as:

$$f\left(\frac{Y_2}{Y_1}, \frac{h_j}{Y_1}, \frac{E_L}{E_1}, \frac{L_r}{Y_2}, \frac{L_j}{Y_1}, \frac{Y_c}{S_l}, \frac{S_w}{S_h}, \frac{V_1^2}{gY_1}, \frac{\rho V_1 Y_1}{\mu}, \frac{\varepsilon}{Y_1}, \frac{H}{r}\right)=0 \quad (2)$$

All variables involved in the phenomenon are incorporated and represented as a function in eqn. (1) using a dimensional analysis approach. Various dimensionless groups (parameters) are derived from these variables, as shown in eqn. (2). Among them, Y_2/Y_1, E_L/E_1, L_j/Y_1, L_r/Y_2 and Y_c/S_l are dependent parameters, influenced by changes in velocity (discharge), while F_{r1}, R_{e1}, μ, g, ρ, ε and n_s are independent parameters. A relationship is established with approach Froude number and incoming Reynolds number for different hydraulic jump characteristics in MSS with reflector. For instance, the sequent depth ratio can be expressed in terms of dynamic viscosity as follows.

$$\frac{Y_2}{Y_1}=0.25\times f\left(\frac{S_w}{S_h}, \frac{Y_c}{S_l}\frac{V_1^2}{gY_1}, \frac{\rho V_1 Y_1}{\mu}, \frac{H}{r}\right) \quad (3)$$

The remaining flow parameters can be similarly represented as shown in eqn. (3). Due to experimental constraints, the influence of surface roughness was not included in these groupings. Eqns. (4) - (7) present the developed empirical models for all flow characteristics. Fig. 7(a) - (d) to Fig. 9(a) - (d) illustrates the best-fit models along with their corresponding R^2 values.

$$\frac{Y_2}{Y_1}=1.137\times\ln\left(\frac{S_w}{S_h}\times\frac{Y_c}{S_l}\times\frac{F_{r1}^2}{R_{e1}}\times\frac{H}{r}\right)+8.5 \quad R^2=0.8955 \quad (4)$$

$$\frac{E_L}{E_1}=0.573\times\ln\left(\frac{S_w}{S_h}\times\frac{Y_c}{S_l}\times\frac{F_{r1}}{R_{e1}^{0.5}}\times\frac{H}{r}\right)-0.18 \quad R^2=0.9606 \quad (5)$$

$$\frac{L_j}{Y_1}=10214\times\left(\frac{S_w}{S_h}\times\frac{Y_c}{S_l}\times\frac{F_{r1}^{0.7}}{R_{e1}}\times\frac{H}{r}\right)-0.3 \quad R^2=0.8602 \quad (6)$$

$$\frac{L_r}{Y_2}=5.5\times\left(\frac{S_w}{S_h}\times\frac{Y_c}{S_l}\times\frac{F_{r1}^{0.5}}{R_{e1}^{0.5}}\times\frac{H}{r}\right)^{-0.5} \quad R^2=0.6721 \quad (7)$$

6. ANFIS (ADAPTIVE NEURO-FUZZY INFERENCE SYSTEM) ANALYSIS

The ANFIS model is utilized for the analysis of flow over MSS models (Model-1, Model-2 and Model-3), incorporating ten input parameters; Y_1 (as in1), Y_2 (as in2), V_1 (as in3), V_2 (as in4), Q (as in5), F_{r1} (as in6), E_1 (as in7), E_2 (as in8), L_r (as in9) and L_j (as in10) with E_L/E_1 or L_j/Y_1 (as out1) designated as the output. The interaction of membership functions among the ten input variables influences the degree of rule activation. When an input value intersects with multiple membership functions, the associated rule exhibits increased activation strength, resulting in a weighted influence on

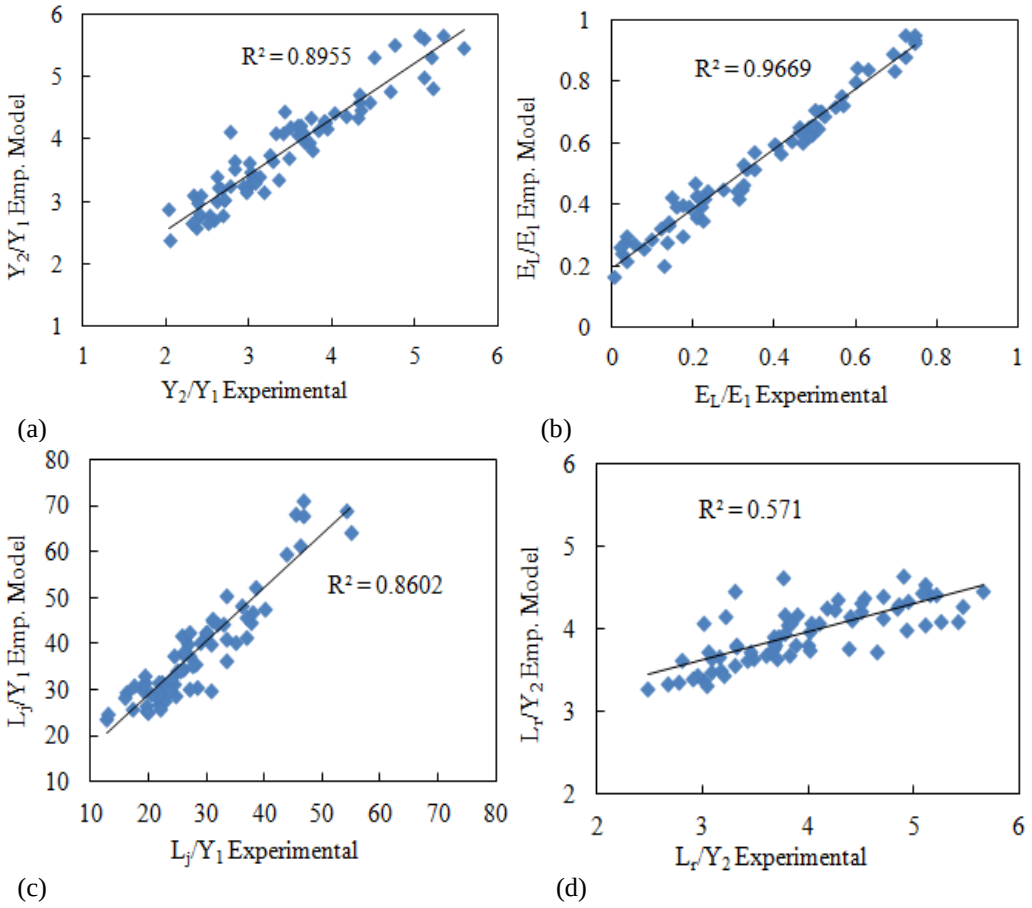

Fig. 8 (a) - (d) Empirical models and their linear fit for model-2

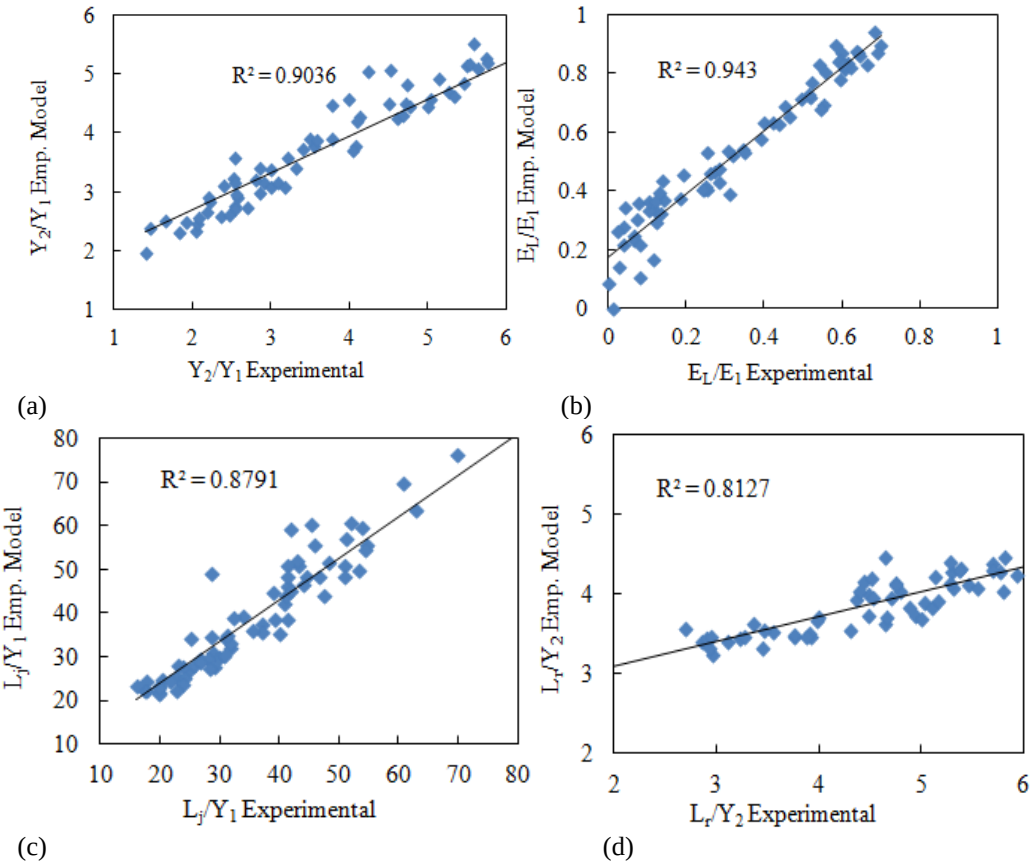

Fig. 9 (a) - (d) Empirical models and their linear fit for model-3

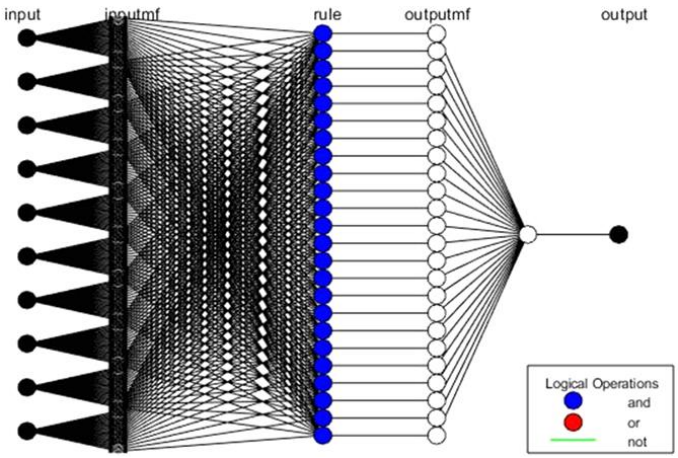

Fig. 10 ANFIS model with ten input parameters and E_L/E_1 or L_j/Y_1 as output parameter

the final output. This fuzzy inference mechanism facilitates smooth interpolation between varying conditions avoiding abrupt transitions. ANFIS architecture consists of a five-layer structure (Fig. 10); first is the input layer, second layer utilizes fuzzy membership functions for these inputs. The system processes 24 fuzzy rules in the third layer, denoted by blue nodes with logical operations (AND/OR). The fourth layer assesses the contribution of each rule by green lines via the output membership functions, while the final fifth layer calculates the singular output (E_L/E_1 or L_j/Y_1). Here, operator AND/OR are represented and incorporate in the rule sections, only one is visible. ANFIS primarily uses AND (e.g., product or minimum T-norm) and OR (e.g., probabilistic sum S-norm) operators in its standard architecture. The "not" operator can be manually incorporated via complementary membership functions (MFs), it is not explicitly represented as a standalone node but it modifies the firing strength of rules by inverting membership degrees. Unlike explicit AND/OR nodes, "not" operations are handled through parameter adjustments in antecedent MFs or rule weights.

6.1 Relative Energy Loss (E_L/E_1)

The ANFIS model is utilized for incorporating ten input parameters; Y_1, Y_2, V_1, V_2, Q, F_{r1}, E_1, E_2, L_r, and L_j with E_L/E_1 as the output for flow over MSS Model-1, Model-2 and Model-3. The analysis is carried out using sub-clustering with range of influence as 0.5, squash factor 1.25, accept and reject ratio 0.5 and 0.15 respectively. The ANFIS structure comprises 541 nodes, including 264 linear parameters and 480 nonlinear parameters, resulting in a total of 744 parameters, which reflects the model's complexity. The system utilizes 50 data pairs for training, lacking distinct validation data pairs, and employs 24 fuzzy rules to define the relationships between inputs and outputs.

Figure 11 illustrates the rule visualization of the ANFIS model, displaying 24 fuzzy rules that establish the relationship between 10 input parameters (in1 to in10) and one output (out1). Each column represents a distinct input variable, while each row denotes a unique rule. The yellow areas in each small graph represent the degree of membership of a specific input value within a fuzzy set, whereas the red vertical line denotes the particular input value under evaluation. The black curves illustrate the membership functions linked to each rule, defining the influence of input values on rule activation. Each rule specifies a distinct set of input conditions that result in a particular output response. The rules function according to fuzzy logic principles, wherein various input conditions are integrated using logical operators (e.g., AND, OR) to ascertain the final output via fuzzy inference. The blue-highlighted areas in the output column represent the predicted output values corresponding to each rule, illustrating the influence of various input conditions on the final ANFIS model prediction. The variation in the yellow-shaded areas across different rules demonstrates the interaction of input variables, highlighting nonlinear dependencies.

Rule 1 illustrates an example in which low values of in1, in2 and in3, when combined with high values of in6 and in9, yield a specific output. Rule 10 illustrates an alternative scenario in which a moderate value of in4, combined with low in7 and high in8, results in a different output. The rules facilitate the ability of ANFIS model to generalize input-output relationships across various scenarios, thereby ensuring precise predictions for complex systems, including flow over MSS for Model-1, Model-2 and for Model-3.

Figure 12(a)–(d) depict three-dimensional surface plots produced by ANFIS model which illustrate the correlation between various input variables and the output variable (E_L/E_1). Figure 12(a) illustrates the correlation between in1 (Y_1, the upstream flow depth) and in6 (F_{r1}, Froude number) with the output variable out1 (E_L/E_1, Relative Energy Loss). The surface exhibits a pronounced increase in E_L/E_1 as F_{r1} rises and Y_1 decreases. This shows that an increase in the velocity of flow (Froude number) there is an increase in energy loss which indicates that considered models-1, 2 and 3 are more effective at higher value of discharge. Also, eqn. (5) with R^2=0.9606 holds good for determining amount of energy loss as it represents significantly for models-4, 5 and 6 together with good R^2 values of 0.9735, 0.9669 and 0.9430 respectively. Figure 12(b) shows the interaction between in1 (Y_1, the upstream flow depth)

Fig. 11 Rule visualization of the ANFIS model for relative energy loss

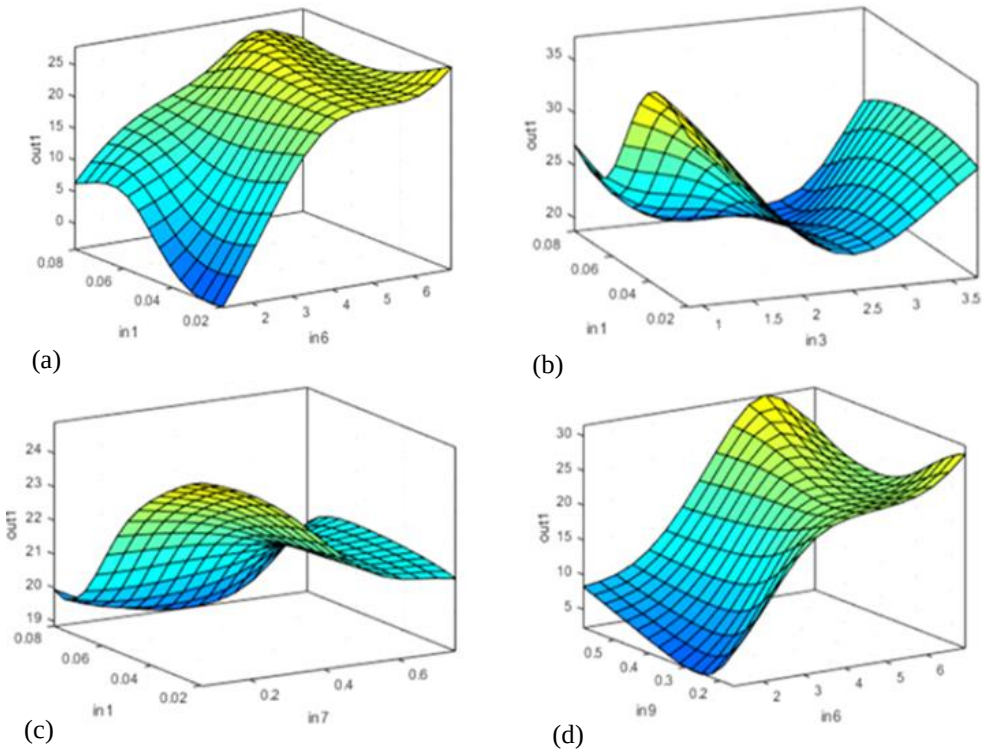

Fig. 12 (a) - (d) Three-dimensional surface plots of ANFIS model for E_L/E_1

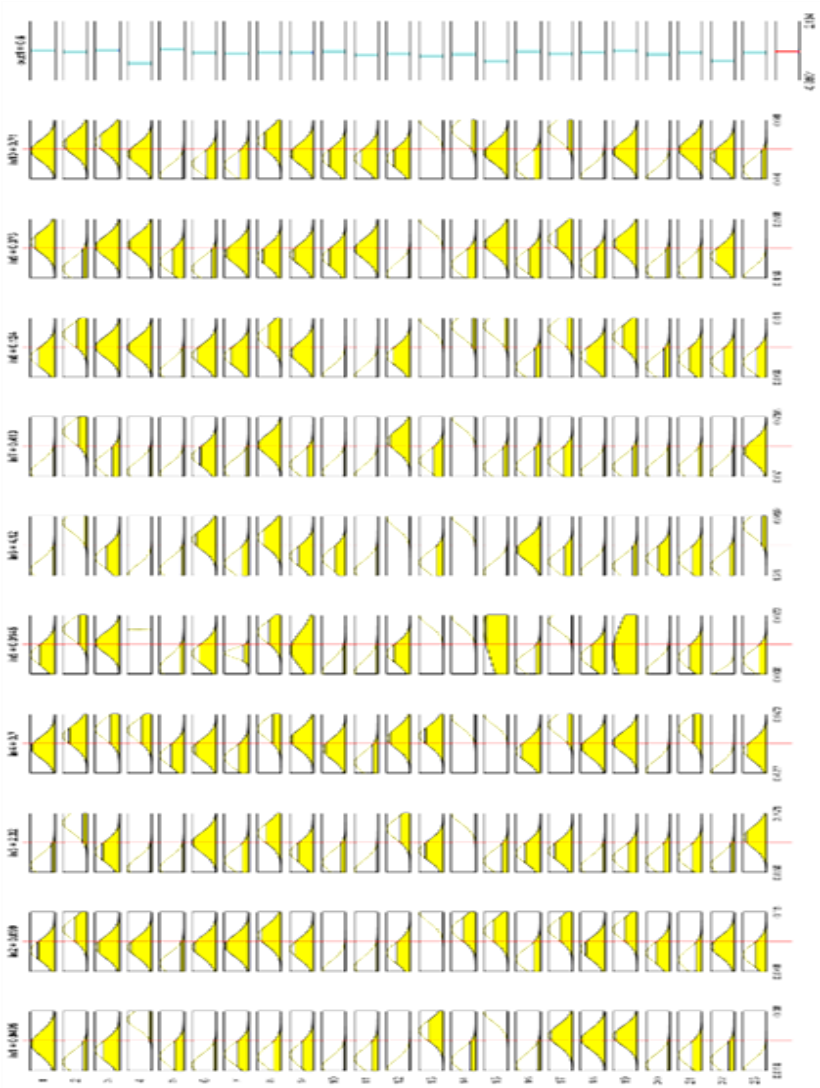

Fig. 13 Rule visualization of the ANFIS model for relative length of jump

and in3 (V_1, velocity before the jump) with the output variable out1 (E_L/E_1, Relative Energy Loss). The surface exhibits a complex pattern characterized by multiple peaks and valleys, indicating a nonlinear relationship between velocity and flow depth. Peaks and valleys indicate variations that distinct flow regimes due to side wave formation and air entrapment in the curved part of stepped spillway and hence affect significant energy dissipation. Similar interpretations were given by Roushangar et al. (2014) and Zounemat-Kermani et al. (2013).

Figure 12(c) illustrates the relationship between in1 (Y_1, the upstream flow depth) and in7 (E_1, energy before the jump). The surface exhibits a more stable trend relative to the prior figures. Stable trend of E_L/E_1 indicates that E_1 has less impact on energy loss in comparison with Y_1 which additionally influences the response. It shows that MSS have important role as soon as flow passes over it. Figure 12(d) illustrates the influence of in9 (L_r, length of roller) and in6 (F_{r1}, Froude number) on the out1 (E_L/E_1). The surface demonstrates a pronounced upward trend, particularly at elevated F_{r1}. This indicates surface roughness has no role on energy dissipation at higher velocity of flow as it overcomes its influence at such velocity of flow.

6.2 Relative Length of Jump (L_j/Y_1)

The ANFIS model is utilized for incorporating ten input parameters; Y_1, Y_2, V_1, V_2, Q, F_{r1}, E_1, E_2, L_r and L_j with L_j/Y_1 as the output for flow over MSS Model-1, Model-2 and Model-3. Figure 13 illustrates the fuzzy rule visualization for the ANFIS model, with the output parameter denoted as L_j/Y_1. Each column represents one of the ten input variables Y_1, Y_2, V_1, V_2, Q, F_{r1}, E_1, E_2, L_r and L_j whereas the rows denote the 23 fuzzy rules that dictate the behavior of the system. The final column in the figure illustrates the predicted output L_j/Y_1, with blue bars indicating the contribution of each fuzzy rule to the overall output value. The red horizontal line in this column indicates the predicted value. The visualization illustrates the model's dependence on nonlinear relationships, evidenced by the notable variation in the shapes and positions of the membership functions. The statistics for the ANFIS model indicate that it consists of 519 nodes and 713 parameters, including 253 linear and 460 nonlinear parameters. The model was trained using 50 data pairs, but it lacks any validation data pairs.

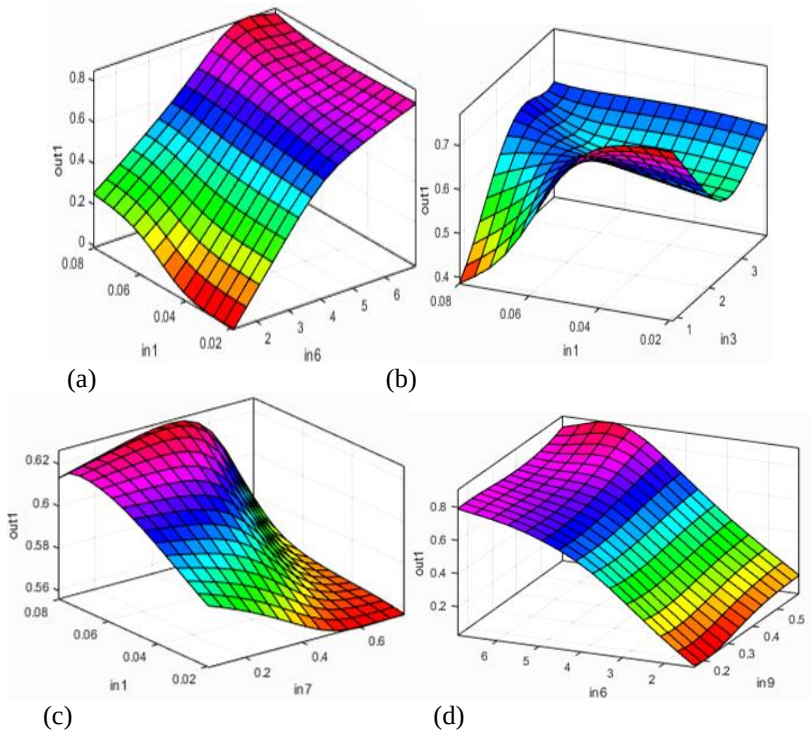

Fig. 14 (a) - (d) Three-dimensional surface plots of ANFIS model for L_j/Y_1

Graphical representation in Fig. 13 illustrates the integration of fuzzy logic and neural networks in ANFIS to establish complex input-output relationships in flow modeling for stepped spillway. The distribution of membership functions and the differing heights of the output bars indicate that several fuzzy rules affect the prediction, facilitating a seamless and continuous mapping of inputs to outputs. This visualization offers a detailed understanding of the ANFIS operation and its effectiveness in predicting hydraulic parameters.

Figure 14(a) - (d) shows set of 3D surface plots demonstrates the parametric impact of different input variables on the output L_j/Y_1 (out1) within the ANFIS modeling framework. Figure 14(a) illustrate the relationships between input parameters in1 (Y_1), in6 (F_{r1}) and output parameter as out1 (L_j/Y_1). The trends demonstrate a nonlinear increasing trend and it becomes constant at higher F_{r1}. Figure 14(b) shows variation of out1 (L_j/Y_1) against in1 (Y_1) and in3 (V_1). It illustrates that at higher depth and low velocity, length of jump increases were as it becomes insignificant at low depth and higher velocity due to impact of curved shaped spillway which controls and reduce the flow energy. It is concluded that L_j/Y_1 indicates high sensitivity towards F_{r1} (or V_1).

Figure 14(c) illustrates the influence of in1 (Y_1) and in7 (E_1) on out1 (L_j/Y_1). Here, the surface demonstrates curvature of falling trend; it indicates as the energy of the flow reduces jump length also reduces effectively. Figure 14(d) represents substantial dependency of out1 (L_j/Y_1) on in6 (F_{r1}) and in9 (L_r). It indicates L_r and L_j are directly dependant variables and both of them exceptionally follow F_{r1} also. Considered three models1, 2 and 3 optimizes the flow and efficient in controlling the length of roller and length of jump. The visualizations provide a thorough understanding of the parametric dependencies within the ANFIS model, facilitating the identification of key input factors that influence L_j/Y_1 in hydraulic modeling. Ouput results are very much allied with Mojtahedi et al. (2020) for length of jump.

7. PERFORMANCE METRIC EVALUATION

Following statistical parameters were used as mentioned below in Table 4 to estimate the accuracy of the proposed ANFIS model as shown in Table 4.

The mean squared error (MSE) is a metric used to assess the accuracy of statistical models. Here, 'n' is total number of data points, 'y' is the observed and 'ŷ' is anticipated values. Here, 'ȳ' represents the Mean of the observed values, while 'ỹ' represents the mean of the anticipated values. Here, the subscript 'i' denotes the data point ID. When the model contained no errors, the MSE was zero. The MSE value increased in proportion to the model's inaccuracy. The root means square error (RMSE) is another popular statistic for expressing model accuracy. The proposed method uses the same units as the data, which makes it easier to analyze and discuss the results. The optimal RMSE value is 0, which indicates a flawless model. The coefficient of determination (R^2) evaluates the model's ability to accurately predict the observed values. R^2 values vary from 0 to 1, with 1 representing a perfect linear relationship between the observed and predicted values.

8. DISCUSSION OF ENERGY DISSIPATION

During these experiments, it was found that the energy dissipation through MSS was improved with more number of steps by controlling the flow rate (Fig. 4), which is in consistent with the previous studies. This might be because of the fixed step dimension, for which

Table 4 Performance index of ANFIS prediction model

Statistical parameter	Cross-validation	Expression	Obtained Values	Desired Value
RMSE	Training	$\sqrt{\sum_{i=1}^{n}\frac{\left(y_i-\hat{y}_i\right)^2}{n}}$	0.062	As less as possible
	Validation		0.121	
	Testing		0.116	
R^2	Training	$\left(\frac{\sum_{i=1}^{n}\left(y_i-\bar{y}_i\right)\left(y_i-\bar{\hat{y}}_i\right)}{\sqrt{\sum_{i=1}^{n}\left(y_i-\bar{y}_i\right)^2\sum_{i=1}^{n}\left(y_i-\bar{\hat{y}}_i\right)^2}}\right)^2$	0.986	Close to one
	Validation		0.969	
	Testing		0.963	
MSE	Training	$\frac{1}{n}\sum_{i=1}^{n}\left(y_i-\hat{y}_i\right)^2$	0.443	Close to zero

specific flow has to undergo for a particular depth and drop ratio. With more number of steps, larger is the energy dissipation due to more water drop and surface friction. The energy dissipation rate can further be improved by varying step height proportion for higher flow rate. Water that falls freely on curved steps splits into two parts: 'top water layer', which flows towards the curved profile and follow next step and responsible for significant hydraulic jump formation, and 'lower back water', which flows to back and strikes the step rise following air entrapment and roller formation. This creates circulation, turbulence and side waves formation (at higher discharge) in response to the flow. When lower back water occurs, typical curve shape helps in dissipating maximum energy of flow within that step of spillway leaving very less residual energy to further dissipate in subsequent steps. Study conducted shows that the energy dissipation rate increases with increasing flow rate as clear in Fig. 4 and Fig. 12(a)-(d). This could be because of increase in lower back water flow rate with discharge. Since the curved step decreases the gap between the lower back water surface and the bottom of the incoming layer, energy dissipation further increases. Backwater might then strike the incoming flow pushing it to the next step by raising water to the top edge of curved step and reducing the critical condition of flow which having large energy. Moreover, as the discharge increases, the free fall disappears and turbulence was generated due to reflectors which leads to formation of skimming flow the steps. The energy dissipation and the residual energy were taken place in subsequent steps ahead. Such method of energy dissipation becomes more beneficial where baffle blocks or sills are not possible to integrate with stilling basins.

Further, curved stepped spillway gives more structural stability to stilling basin by dissipating most of the energy through back water flow in steps and low energy only remains at stilling basin for bed erosion. This configuration of reflectors controls the symmetry of water distribution and increased the air entrainment effectively as shown in Fig. 2(c). These steps have a vertical curvature and hence disturb the flow more and behave as reflectors that direct water flow over the steps. The new step configurations with reflectors dissipated energy more effectively. They also reduced the residual energy, roller length and jump length at all flow rates clearly seen in Fig. 4, Fig. 5 and Fig. 6 respectively.

9. EXPERIMENTAL LIMITATIONS

The authors recognize that the results presented are specifically applicable to developing, nonaerated flow due to the scale of the model utilized. Nevertheless, it remains important and beneficial to evaluate the overall impact of the various configurations discussed. The aeration of the flow is anticipated to reduce friction on the spillway because of the entrained air, a consideration that should be taken into account when applying these findings to full-scale spillways. Stepped spillways with reflectors can cause significant local deviations due to backwater effects and turbulence, at this stage influencing parameters becomes non-linear and scale effect leads to instability in exact prediction of characteristics. Since spillways are typically designed for high specific discharges—resulting in higher y_c/S_h values than those employed in this study—the authors still find the results valuable for comparing different step configurations in a controlled environment. The potential impact of scale effects is significant due to the relatively small size of the model compared to actual spillways. This issue has been thoroughly examined by Pfister and Chanson (2014) and other researchers, who investigated how step geometry influences flow aeration in spillways, providing insights into scale effects and key parameters such as Reynolds numbers and their importance in laboratory spillway modeling. Although these parameters would be crucial in any comprehensive study aimed at replicating the findings at full scale, the authors emphasize that their primary objective here is to enhance understanding of how MSS affects energy dissipation.

10. CONCLUSIONS

Following a series of experiments carried out in a 0.2 m wide laboratory flume over a range of discharge rates, it is clear that the rate of energy dissipation depends on the discharge rate and more importantly on the step configuration i.e., n, S_h, S_l, S_w. Since it is important to address unpredictable flow conditions and to provide structural stability of stilling basin, it is recommended to use stepped spillway with curved reflectors rather designing a flat stepped spillway with sharp edges. To the best of our knowledge, information on the performance of these different configurations model is not widely available using ANFIS technique and further work should seek to build on these preliminary results. The key findings from these experiments are as follows:

- There was a clear difference between the steps configurations used in different spillway models in terms of energy dissipation. MSS with a greater number of steps and larger step length dissipates more energy as well as effectively controls the jump length as shown in Fig. 4 and in Fig. 5.
- Empirical models so developed for determining Y_2/Y_1, E_L/E_1, L_j/Y_1 and L_r/Y_2 are greatly influenced by reflectors, back water flow and turbulence.
- Good R^2 values of 0.89, 0.96 and 0.86 for empirical models of Y_2/Y_1, E_L/E_1 and L_j/Y_1 as eqn. 4 to eqn. 6 are obtained. These R^2 values in stepped spillways with reflectors are likely due to the inherent complexity of the flow, limitations of empirical modeling, measurement uncertainties, and unmodeled physical phenomena in such systems. Low R^2 value of 0.67 for L_r/Y_2 is devoted to measurement challenge to turbulence, rollers and eddies formation.
- Excellent correlation between experimental values and values obtained from empirical model (as shown in Fig. 7, Fig. 8 and Fig. 9) for jump characteristics indicates the efficacy of developed model that can be used for future studies.
- ANFIS predicts the non-linear transition effectively which is clear by performance metric evaluation with RMSE, R^2 and MSE training values as 0.06, 0.98 and 0.43 respectively.
- 3D surface plot provides thorough understanding of parametric dependencies of relative energy loss and relative length of jump on E_1, E_2, F_{r1} and L_r.
- Presented work underscores the evolution and optimization of stepped spillway designs to maximize energy dissipation efficiency with MSS for hydraulic engineers.

11. FUTURE DIRECTION

The hydraulic behavior of MSS is complex, involving turbulent, aerated and multi-phase flows. Accurately predicting energy dissipation and jump length is challenging using traditional analytical or empirical methods. Advanced techniques, such as the Adaptive Neuro-Fuzzy Inference System (ANFIS) offer significant advantages even with appurtenance arrangement required for higher discharges over spillway. Complex reflectors and rough bed configurations can be analyzed using data-driven methodologies like hybrid ANFIS, Gene-expression programming, ANN, XGBoost and LightGBM which may result in improved hydraulic performance of such typical structures.

ACKNOWLEDGEMENTS

The authors are thankful to Dr. Yogesh Iyer Murthy (Assistant Professor) and the Civil Engineering Department at JUET Guna, India, for all kind of technical support.

CONFLICT OF INTEREST

The authors have no conflicts to disclose.

AUTHORS CONTRIBUTION

Prachi Dharmadhikari: Methodology – Validation – Formal Analysis – Data Curation – Writing – Original Draft – Visualisation. **Sumit Gandhi:** Conceptualization – Methodology – Writing – Review & Editing – Supervision.

REFERENCE

Alashan, S., İkincioğulları, E., & Yalçın, E. E. (2023). Practical design of stepped spillways using fuzzy inference system. *Preprint, Version 1, Research Square*, https://doi.org/10.21203/rs.3.rs-2937963/v1.

Albank, H. H., & Khassaf, S. I. (2023). An experimental investigation of energy dissipation for stepped spillways with different flow conditions. *Mathematical Modelling of Engineering Problems, 10*(1), 340–346. https://doi.org/10.18280/mmep.100139.

Al-Husseini, T. R., Ghawi, A. H., & Ali, A. H. (2019). Performance of hydraulic jump rapid mixing for enhancement of turbidity removal from synthetic wastewater: A comparative study. *Journal of Water Process Engineering, 30*, 100590. https://doi.org/10.1016/j.jwpe.2018.03.005

Aminpour, Y., & Farhoudi, J. (2017). Similarity of local scour profiles downstream of stepped spillways. *International Journal of Civil Engineering, 15*(5), 763–774. https://doi.org/10.1007/s40999-017-0168-9.

Asadi, E., Dalir, A. H., Farsadizadeh, D., Hassanzaheh, Y., & Salmasi, F. (2015). Energy dissipation of skimming flow with different sill dimensions in stepped spillway model. *International Journal of Agriculture and Biosciences, 4*(3), 118–121. https://www.ijagbio.com/pdf-files/volume-4-no-3-2015/118-121.pdf

Boes, R. M., & Hager, W. H. (2003). Hydraulic design of stepped spillways. *Journal of Hydraulic Engineering, 129* (9), 671–679. https://doi.org/10.1061/(ASCE)0733-9429(2003)129:9(671)

Bushra, A., & Afzal, N., (2006). Hydraulic jump in circular and U-shaped channels. *Journal of Hydraulic Research, 44*(4), 567–576, https://doi.org/10.1080/00221686.2006.9521707

Chanson, H. (2001). Hydraulic design of stepped spillways and downstream energy dissipaters. Dam Engineering, 11 (4), 205–242. (ISSN 0 617 00563 X).

Chanson, H. (1994). Comparison of energy dissipation between nappe and skimming flow regimes on

stepped chutes. *Journal of Hydraulic Research*, *32*(2), 213–218. https://doi.org/10.1080/00221686.1994.10750036.

Chanson, H. (1996). Prediction of the transition nappe/skimming flow on a stepped channel**.** *Journal of Hydraulic Research*, *34***(**3), 421–429. https://doi.org/10.1080/00221689609498490

Daneshfaraz, R., Sadeghi, H., Ghaderi, A., & Abraham, J. P. (2024). Characteristics of hydraulic jump and energy dissipation in the downstream of stepped spillways with rough steps. *Flow Measurement and Instrumentation*, *96*, 102506. https://doi.org/10.1016/j.flowmeasinst.2023.102506

Djamaa, W., Bouchelaghem, D., & Bouchelaghem, M. (2020). Study of the experimental approach of the relative length of the surface roller of the hydraulic jump evolving in rectangular channels with rough beds. *Journal of Fundamental and Applied Sciences*, *12*(3), 1190-1203. 10.4314/jfas.v12i3.13

Eghlidi, E., Barani, G. A., & Qaderi, K. (2020). Laboratory investigation of stilling basin slope effect on bed scour at downstream of stepped spillway: physical modeling of Javeh RCC dam. *Water Resources Management*, *34*(1), 87–100. https://doi.org/10.1007/s11269-019-02395-5.

Elshaarawy, M. K., & Hamed, A. K. (2025). Modeling hydraulic jump roller length on rough beds: A comparative study of ANN and GEP models. *Journal of Umm Al-Qura University for Engineering and Architecture*, *12*(1), 15–30. 10.1007/s43995-024-00093-x

Eltoukhy, M. (2016). Hydraulic jump characteristics for different open channel and stilling basin layouts. *International Journal of Civil Engineering and Technology*, *7*(2), 290–301. https://iaeme.com/MasterAdmin/Journal_uploads/IJCIET/VOLUME_7_ISSUE_2/IJCIET_07_02_025.pdf

Felder, S., & Chanson, H. (2011). Air–water flow properties in stepwise aeration cascades: new physical insights. *Environmental Fluid Mechanics*, *11*(3), 263–288.

Ghaderi, A., Abbasi, S., Abraham, J. & Azamathulla, H. M. (2020). Efficiency of trapezoidal labyrinth shaped stepped spillways, *Flow Measurement and Instrumentation*, *72*, 101711. https://doi.org/10.1016/j.flowmeasinst.2020.101711

Ikinciogullari, E. (2021). Energy dissipation performance of the trapezoidal stepped spillway. *Journal of Engineering Research*, https://doi.org/10.36909/jer.13649.

Kordnaeij, M., Tehrani, M. J. O. M., Pari, S. A. A., & Falahat, H. (2023). *Energy dissipation on stepped spillways: the effect of mounted step roughness*. Proceedings of the 40th IAHR World Congress, 21, 25. https://doi.org/10.3850/978-90-833476-1-5_iahr40wc-p1620-cd

Mero, S., & Mitchell, S. (2017). Investigation of energy dissipation and flow regime over various forms of stepped spillways. *Water and Environment Journal*, *31* (1), 127–137. https://doi.org/10.1111/wej.12224

Mojtahedi, A., Soori, N. & Mohammadian, M. (2020). Energy dissipation evaluation for stepped spillway using a fuzzy inference system. *SN Applied Science 2*, 1466. https://doi.org/10.1007/s42452-020-03258-0

Nasralla T. H. (2021). Energy dissipation in stepped spillways using baffled stilling basins. *ISH Journal of Hydraulic Engineering*, *28* (3), 243–250. https://doi.org/10.1080/09715010.2021.1871786

Nikmehr, S., & Aminpour, Y. (2020). Numerical simulation of hydraulic jump over rough beds. *Periodica Polytechnica Civil Engineering*, *64*(2), 396–407. https://doi.org/10.3311/PPci.15292

Nishank A. & Ellora, P. (2025). Impacts of bed roughness and orientation on hydraulic jump: A review. *Water Science and Engineering, 18* (1), 90-101. https://doi.org/10.1016/j.wse.2024.03.003.

Nouri, M., Sihag, P., Salmasi, F., & Kisi, O. (2020). Energy loss in skimming flow over cascade spillways: Comparison of artificial intelligence-based and regression methods. *Applied Sciences*, *10*(19), 6903. https://doi.org/10.3390/app10196903

Ohtsu, I., Yasuda, Y., & Takahashi, M. (2004). Flow characteristics of skimming flows in stepped channels. *Journal of Hydraulic Engineering*, *130* (9), 860–869. https://doi.org/10.1061/(ASCE)0733-9429(2004)130:9(860)

Parsaie, A., Shareef, S. J. S., Haghiabi, A. H., Irzooki, R. H., & Khalaf, R. M. (2022). Numerical simulation of flow on circular crested stepped spillway. *Applied Water Science*, *12*, 215. https://doi.org/10.1007/s13201-022-01737-w

Parsamehr, M., Sadraddini, A. A., & Ghaderi, A. (2023). Effect of surface roughness and channel slope on hydraulic jump characteristics. *Iranian Journal of Science and Technology, Transactions of Civil Engineering*, *48*, 1695–1713. https://doi.org/10.1007/s40996-023-01246-z

Pegram, G. S., Officer, A. K., & Mottram, S. A. (1999). Hydraulic of skimming flow on modelled stepped spillways. *Journal of Hydraulic Engineering*, *125*(5), 500–510. https://doi.org/10.1061/(ASCE)0733-9429(1999)125:5(500).

Pfister, M., & Chanson, H. (2014). Effect of step geometry on flow aeration on embankment stepped spillways. *Journal of Hydraulic Engineering*, *140*(4), 04014002. https://doi.org/10.1061/(ASCE)HY.1943-7900.0000845

Rajaratnam, N. (1990). Skimming flow in stepped spillway. *Journal of Hydraulic Engineering*, *116*(4),

587–691, https://doi.org/10.1061/(ASCE)0733-9429-(1990)116:4(587).

Roushangar, K., Shiri, J., & Ebrahimi, H. (2014). Modeling energy dissipation over stepped spillways using ANFIS and GEP techniques. *Water Resources Management*, *28*(10), 2865-2880. https://doi.org/10.1016/j.jhydrol.2013.10.053

Saghebian, S. M. (2018). Predicting the relative energy dissipation of hydraulic jump in rough and smooth bed compound channels using SVM. *Water Supply*, *19*(4), 1110–1120. https://doi.org/10.2166/ws.2018.162

Saurabh, P., Vijay, K., Noopur, A., Shailesh, K., Gupta, S., & Anbu, K. (2023). Application of machine learning approaches in the computation of energy dissipation over rectangular stepped spillway. *H2Open Journal*, *6* (3), 433–448. https://doi.org/10.2166/h2oj.2023.007

Salmasi, F., & Abraham, J. (2022). Effect of slope on energy dissipation for flow over a stepped spillway. *Water Supply*, *22*(5), 5056-5069. https://doi.org/10.2166/ws.2022.193

Simsek, O., Akoz, M.S. & Oksal, N.G.S. (2023). Experimental analysis of hydraulic jump at high froude numbers. *Sādhanā 48*, (47). https://doi.org/10.1007/s12046-023-02081-8

Wüthrich, D., & Chanson, H. (2015). Aeration performances of a gabion stepped weir with and without capping. *Environmental Fluid Mechanics*, *15*(4), 711–730. https://doi.org/10.1007/s10652-014-9379-1

Yu, Z., Jianhua W., F. Ma, & Shangtuo, Q. (2021). Experimental Investigation of the Hydraulic Performance of a Hydraulic-Jump-Stepped Spillway, *KSCE Journal of Civil Engineering, 25* (10), 3758-3765. https://doi.org/10.1007/s12205-021-1709-y

Zounemat-Kermani, M., Kisi, O., & Roushangar, K. (2013). Modeling of air demand in bottom outlet using adaptive neuro-fuzzy inference system. *Journal of Hydraulic Research*, *51*(1), 96-101.

Zuhaira, A. S., Salmasi, F., & Abraham, J. (2020). Numerical investigation of step dimensions impact over gabion stepped spillways. *International Journal of Civil Engineering and Technology*, *11*(5), 1–12.